ISBN: 978-3-95450-132-8 doi:10.18429/JACoW-IPAC2014-WEPRO053

ALL-OPTICAL FREE-ELECTRON LASERS USING TRAVELING-WAVE THOMSON-SCATTERING

K. Steiniger*, A. Debus, A. Irman, A. Jochmann, R. Pausch, U. Schramm, T. Cowan and M. Bussmann, Helmholtz-Zentrum Dresden-Rossendorf (HZDR), 01314 Dresden

Traveling-Wave Thomson-Scattering (TWTS) [1–3] is a scheme for the realization of compact optical undulators. TWTS utilizes high-power, short-pulse lasers providing sub-mm undulator periods. These allow for operation of an X-ray light source at Å wavelength with only a few hundred MeV electron energy. Here, we show that by carefully controlling dispersion of a TWTS laser pulse it is possible to achieve free-electron laser (FEL) operation, creating a TWTS optical FEL (OFEL). The electron energies needed for X-ray radiation are an order of magnitude smaller compared to existing hard-X-ray FELs requiring several GeV [4, 5]. Moreover, with sub-mm undulator wavelengths the FEL process saturates in sub-m interaction distances removing the need for electron beam focusing during the interaction. Using a laser undulator further has the advantage that no material is required for producing or containing the undulator field which become a source of unwanted wakefields when aiming for compact setups.

In Traveling-Wave Thomson-Scattering the interaction distances needed to drive the FEL process until saturation are achieved in two steps. First, by choosing a side-scattering geometry, where laser and electron direction of propagation enclose the interaction angle ϕ. Second, by tilting the laser pulse-front by half of the interaction angle $\alpha_{\text{tilt}} = \phi/2$ for full spatial overlap of the electron bunch with the laser pulse during the entire interaction (Fig. 1). Thereby, the maximum number of undulator periods experienced by the electrons becomes independent of the laser pulse duration which is the limit for head-on Thomson scattering [6,7]. With TWTS the interaction distance is limited by the laser pulse width and thus by the available laser power.

The variability of TWTS with respect to the interaction angle ϕ gives control over the scattered wavelength λ_{FEL} independent of the available electron energy $E_e = \gamma_0 mc^2$ and the laser wavelength λ_0:

$$\lambda_{\text{FEL}} = \frac{\lambda_0(1 + a_0^2/2)}{2\gamma_0^2(1 - \beta_0 \cos\phi)} ,$$

where β_0 is the electron velocity normalized to the speed of light. Depending on the peak intensity I_0 of the laser, an additional redshift in the scattered wavelength is induced through the laser strength parameter $a_0 = \lambda_0\sqrt{I_0/13.7\,\text{GW}}$. TWTS furthermore gives control over the bandwidth of the scattered radiation through the laser pulse width w_0, which determines the number of undulator periods N_{u} experienced by the electrons.

$$\frac{\Delta\lambda}{\lambda} = \frac{1}{N_{\text{u}}} = \frac{\lambda_0}{w_0 \tan(\phi/2)}$$

This possibility makes TWTS interesting for applications where a defined bandwidth is required.

The realization of a TWTS-OFEL requires dispersion controlled laser pulses. Dispersion compensation is needed due to the generation of the required pulse-front tilt in TWTS with an optical grating, which also causes the frequencies in the laser pulse to travel in different directions leading to laser pulse lengthening. This lengthening can become severe thus inhibiting high-gain in the FEL process. Dispersion compensation can be accomplished with an additional grating setup before the pulse-front tilting grating [1, 3].

For the first time, a fully analytic, three-dimensional description of TWTS laser pulses has been developed that allows for optimum control of dispersion to all orders. With this essential ingredient, we could prove that the electron and radiation field dynamics in the TWTS undulator are identical to the the dynamics in a standard magnetic FEL [3]. This work thus goes well beyond previous OFEL models using TWTS scattering geometries [8–10] as it can provide scaling laws for electron and laser beam requirements that allow to find suitable parameters for OFEL operation.

The TWTS-OFEL pendulum and radiation field equations for the electron phase θ in the ponderomotive wave, the scaled electron energy p, the scaled radiation field amplitude α and the radiation field phase Υ are

$$\frac{\mathrm{d}\theta_j}{\mathrm{d}\bar{t}} = p_j \qquad \frac{\mathrm{d}p_j}{\mathrm{d}\bar{t}} = 2\alpha\cos(\theta_j + \Upsilon)$$

$$\frac{\mathrm{d}\alpha}{\mathrm{d}\bar{t}} = \langle\cos(\theta + \Upsilon)\rangle \qquad \frac{\mathrm{d}\Upsilon}{\mathrm{d}\bar{t}} = -\frac{1}{\alpha}\langle\sin(\theta + \Upsilon)\rangle .$$

Where time is measured in gain periods $\bar{t} = ct/L_{\text{G}}\sqrt{3}$, $p_j = (\gamma_0 - \gamma_j)/\rho\gamma_0$ and $\langle\cdot\rangle$ is an average over all the electrons in the bunch. The radiation field amplitude α is scaled to reflect the ratio of the radiated power P to the electron beam power $P_e = \gamma_0 mc^2 I/e$ and is given by $\alpha^2 = P/\rho P_e$. When saturation is reached after roughly 16 gain lengths L_{G}, the scaled radiation field amplitude becomes $\alpha^2 \approx 1$ and thus the radiated power can be approximated with $P \approx \rho P_e$. The power gain length of the TWTS-OFEL is

$$L_{\text{G}} = \frac{\lambda_0}{4\pi\sqrt{3}(1 - \beta_0\cos\phi)\rho} ,$$

which is similar to standard magnetic FELs with the only difference arising from the effective undulator period $\lambda_{\text{u}} = \lambda_0/(1 - \beta_0\cos\phi)$ experienced by the electrons due to the side-scattering geometry. The corresponding Pierce parameter of the TWTS-OFEL also takes the same form as in a

* k.steiniger@hzdr.de

ISBN: 978-3-95450-132-8 doi:10.18429/JACoW-IPAC2014-WEPRO053

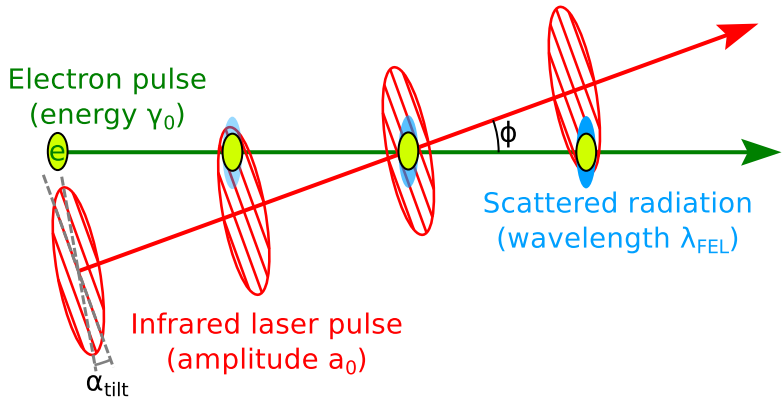

Figure 1: Traveling-Wave Thomson-Scattering (TWTS) utilizes pulse-front tilted high-power laser pulses to maximize the interaction distance in the scattering of relativistic electrons. The pulse-front tilt angle is chosen to provide continuous spatial overlap of the laser pulse with the electrons during the interaction. In this way, the possible interaction distance becomes independent of the laser pulse duration and is instead only limited by the laser pulse width and thus by the available laser power. The interaction distances achieved are suitable for the realization of an optical free-electron laser (OFEL).

magnetic undulator

$$\rho = \left[\frac{1}{16\gamma_0^3} \frac{I}{I_A} \left(\frac{\lambda_0 a_0 f_B}{2\pi\sigma_e (1 - \beta_0 \cos\phi)} \right)^2 \right]^{1/3} ,$$

with the electron beam peak current I, the electron beam rms cross-sectional radius σ_e, the Bessel function factor $f_B = [J_0(\chi) - J_1(\chi)]$ with $\chi = a_0^2/(2 + a_0^2)$ and the Alfvén current $I_A = 4\pi\varepsilon_0 mc^3/e \approx 17\,\mathrm{kA}$.

The essential scaling laws for the electron and laser beam requirements to realize a TWTS-OFEL are

$$\frac{\Delta\gamma_0}{\gamma_0} \leq \rho \propto \gamma_0^{1/3} \lambda_{FEL}^{2/3} , \quad (1)$$

$$\epsilon_N \leq \sigma_e \sqrt{2\rho} \propto \left[\gamma_0^{1/3} \lambda_{FEL}^{2/3} \right]^{1/2} , \quad (2)$$

$$\epsilon_N \leq \frac{2\gamma_0 \sigma_e^2}{L_{int}} \propto \gamma_0^{-2/3} \lambda_{FEL}^{-1/3} \text{ and} \quad (3)$$

$$P_L\,[TW] = 34.29 \times 10^{-3} \sigma_e \frac{a_0^2}{\lambda_0^2} L_{int} \sin\phi . \quad (4)$$

These are deduced from the FEL gain bandwidth $\Delta\lambda_{FEL}/\lambda_{FEL} = 2\rho$ together with the expression for the scattered FEL wavelength λ_{FEL} [3].

The first requirement (1) gives an upper limit on the electron beam energy spread $\Delta\gamma_0/\gamma_0$. This limit ensures that all electrons are radiating within the gain bandwidth. Its scaling proportional to $\gamma_0^{1/3} \lambda_{FEL}^{2/3}$ shows that the maximum allowed electron energy spread becomes smaller when aiming for more compact setups, i. e. the chosen target wavelength remains constant but the undulator period and electron energy is reduced. This is a general property of compact FEL schemes and not unique to TWTS. The smaller the undulator period and the required energy becomes for a given target wavelength, the more the quality of the electron beam has to be increased, since with less electron energy less radiation is produced and sufficient gain is only achieved when the scattering bandwidth becomes smaller.

The second requirement (2) takes broadening of the bandwidth due to divergence of the electron beam into account. Electrons propagating under an angle to the central orbit of the electron bunch radiate at a different wavelength due to a different undulator period in this direction and a different observation angle of the radiation [11]. The result is an upper limit on the normalized electron beam emittance ϵ_N.

Moreover, an increase in emittance causes a defocusing of the electron beam during the interaction, resulting in a reduced spatial overlap between the electron and laser pulse, thereby degrading the gain. The third requirement (3) ensures optimum spatial overlap and sets another limit on the normalized electron beam emittance.

The required laser power P_L for full spatial overlap of electron and laser pulse is given in (4).

Comparing the two emittance requirements and the required laser power, it becomes clear that the interaction angle can be used to minimize the requirements on the electron beam parameters while trying to stay close to an available laser system. This minimization requires either the electron energy or the target wavelength to be chosen while the other one remains free. The first of these two options represents an optimization strategy for a proof-of-principle experiment at an existing facility and the second option corresponds to a dedicated design of a new light source. For most experimental realizations, the emittance criterion will however be the toughest requirement to meet.

The combination of laser wakefield acceleration (LWFA) of electrons and a laser undulator allows for ultra-compact all-optical FELs. Additionaly, the experimental realization of a TWTS-OFEL with LWFA electrons offers inherent synchronization of electrons and laser pulse when using the same laser as the driver of the electron source and the optical undulator.

ISBN: 978-3-95450-132-8 doi:10.18429/JACoW-IPAC2014-WEPRO053

Table 1: An all-optical TWTS free-electron laser example scenario using LWFA electrons in comparison to the LCLS conventional magnetic FEL. The laser wavelength is $\lambda_0 = 1\,\mu m$ and the electron rms cross-sectional radius $\sigma_e = 11\,\mu m$.

Parameter	TWTS-OFEL	LCLS
Resonant Wavelength [Å]	1.5	1.5
Interaction angle [°]	5	-
Undulator period [mm]	0.26	30.0
Electron energy [GeV]	0.46	13.6
Peak current [kA]	5	3.5
Norm. emittance [mm mrad]	0.24	0.5
Rel. energy spread	0.02 %	0.01 %
Undulator parameter a_0 or K	0.2	3.5
Laser power [PW]	1.1	-
Gain length [m]	0.05	3.5
Interaction distance [m]	0.8	132
Peak X-ray power [GW]	0.5	40

Currently, LWFA experiments do not yet reach the required relative energy spreads and shot-to-shot stability in combination with bunch charges of at least 10 pC. Relative energy spreads are at the moment at a percent level [12–14] but improvements are expected from approaches allowing better control of the injection process, such as colliding pulse schemes [15] or ionization injection [16].

Despite these current limitations, LWFA provides for normalized emittances down to 0.1 mm mrad [17–21] and high peak currents of several kA resulting from the ultra-short electron bunch durations of a few fs [22–25]. Thus LWFA is an ideal source for driving TWTS-OFELs, as electron energies of a few hundred MeV to GeV needed for operation of an X-ray light source have been shown repeatedly [26, 27].

An example scenario of an all-optical TWTS free-electron laser radiating at 1.5 Å wavelength is given in table 1 and compared to the Linac Coherent Light Source (LCLS) [4]. The comparison shows that an all optical TWTS-OFEL radiating at the same wavelength can be realized with an order of magnitude smaller electron energy of 460 MeV and within a two orders of magnitude smaller interaction distance of 78 cm. Numerical integration of the electron and radiation field equations shows that the radiated power saturates after this distance at about 500 MW (Fig. 2).

To conclude, with Traveling-Wave Thomson-Scattering (TWTS) optical free-electron lasers can be realized. A TWTS-OFEL operated in the X-ray range with state of the art laser systems requires electron sources providing high quality electron beams with very low emittances. This is a general characteristic of compact FEL concepts and not unique to TWTS-OFELs. However, with improving the field quality and stability of existing petawatt laser sources, restrictions on the emittance can be loosened, paving the way towards a realization of compact TWTS-OFELs at existing electron accelerator facilities.

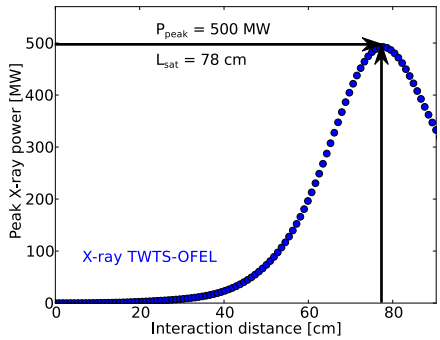

Figure 2: Gain curve of the all-optical TWTS free-electron laser X-ray example from table 1 using LWFA electrons. The increase in peak X-ray power during the interaction is obtained from numerical integration of the TWTS-OFEL pendulum and radiation field equations of motion. The radiated power saturates at about 500 MW within an interaction distance of 78 cm. The small undulator period of only 0.26 mm allows for such a short saturation distance. The simulation used 1000 electrons with an initial relative energy spread of 0.02 % and a random distribution in initial pondermotive wave phase in $\theta_j \in [0, 2\pi]$.

The presented example shows how an ultra-compact TWTS-OFEL could be realized with a well controlled laser wakefield accelerator. The combination of TWTS and laser wakefield acceleration (LWFA) offers inherent synchronization of laser and electron pulse and profits from the ultra-low emittances and ultra-short electron bunch durations available with LWFA. These all-optical TWTS-OFELs would provide "table-top" sources of high-brightness, spatially and temporally coherent X-ray radiation pulses with femtosecond pulse durations that could be used to resolve ultra-fast processes at atomic scales in solid-density materials.

ISBN: 978-3-95450-132-8 doi:10.18429/JACoW-IPAC2014-WEPRO053

REFERENCES

[1] Debus, A. *et al.* Traveling-wave Thomson scattering and optical undulators for high-yield EUV and X-ray sources. *Applied Physics B: Lasers and Optics* **100**, 61–76 (2010). 10.1007/s00340-010-3990-1.

[2] Steiniger, K. *et al.* Wave optical description of the Traveling-Wave Thomson-Scattering optical undulator field and its application to the TWTS-FEL. *Nuclear Instruments and Methods in Physics Research Section A: Accelerators, Spectrometers, Detectors and Associated Equipment* (2013).

[3] Steiniger, K. *et al.* Optical Free-Electron Lasers with Traveling-Wave Thomson-Scattering. Submitted to Journal of Physics B: Atomic, Molecular and Optical Physics (2014).

[4] Emma, P. *et al.* First lasing and operation of an ångstrom-wavelength free-electron laser. *Nature Photonics* **4**, 641–647 (2010).

[5] Ishikawa, T. *et al.* A compact X-ray free-electron laser emitting in the sub-angstrom region. *Nature Photonics* **6**, 540–544 (2012).

[6] Esarey, E., Ride, S. K. & Sprangle, P. Nonlinear Thomson scattering of intense laser pulses from beams and plasmas. *Phys. Rev. E* **48**, 3003–3021 (1993).

[7] Debus, A. *et al.* Linear and Non-Linear Thomson-Scattering X-Ray Sources Driven by Conventionally and Laser Plasma Accelerated Electrons. *Proc. of SPIE* **7359**, 735908 (2009).

[8] Andriyash, I. A., d'Humières, E., Tikhonchuk, V. T. & Balcou, P. X-Ray Amplification from a Raman Free-Electron Laser. *Phys. Rev. Lett.* **109**, 244802 (2012).

[9] Chang, C., Tang, C. & Wu, J. High-Gain Thompson-Scattering X-Ray Free-Electron Laser by Time-Synchronic Laterally Tilted Optical Wave. *Phys. Rev. Lett.* **110**, 064802 (2013).

[10] Lawler, J. E. *et al.* Nearly copropagating sheared laser pulse FEL undulator for soft x-rays. *Journal of Physics D: Applied Physics* **46**, 325501 (2013).

[11] Ride, S. K., Esarey, E. & Baine, M. Thomson scattering of intense lasers from electron beams at arbitrary interaction angles. *Physical Review E* **52**, 5425–5442 (1995).

[12] Banerjee, S. *et al.* Stable, tunable, quasimonoenergetic electron beams produced in a laser wakefield near the threshold for self-injection. *Phys. Rev. ST Accel. Beams* **16**, 031302 (2013).

[13] Osterhoff, J. *et al.* Generation of Stable, Low-Divergence Electron Beams by Laser-Wakefield Accelerationin a Steady-State-Flow Gas Cell. *Phys. Rev. Lett.* **101**, 085002 (2008).

[14] Karsch, S. *et al.* GeV-scale electron acceleration in a gas-filled capillary discharge waveguide. *New Journal of Physics* **9**, 415 (2007).

[15] Rechatin, C. *et al.* Controlling the Phase-Space Volume of Injected Electrons in a Laser-Plasma Accelerator. *Phys. Rev. Lett.* **102**, 164801 (2009).

[16] Clayton, C. E. *et al.* Self-Guided Laser Wakefield Acceleration beyond 1 GeV Using Ionization-Induced Injection. *Phys. Rev. Lett.* **105**, 105003 (2010). URL `http://link.aps.org/doi/10.1103/PhysRevLett.105.105003`

[17] Plateau, G. R. *et al.* Low-Emittance Electron Bunches from a Laser-Plasma Accelerator Measured using Single-Shot X-Ray Spectroscopy. *Phys. Rev. Lett.* **109**, 064802 (2012).

[18] Kneip, S. *et al.* Characterization of transverse beam emittance of electrons from a laser-plasma wakefield accelerator in the bubble regime using betatron X-ray radiation. *Phys. Rev. ST Accel. Beams* **15**, 021302 (2012).

[19] Weingartner, R. *et al.* Ultralow emittance electron beams from a laser-wakefield accelerator. *Phys. Rev. ST Accel. Beams* **15**, 111302 (2012). URL `http://link.aps.org/doi/10.1103/PhysRevSTAB.15.111302`

[20] Brunetti, E. *et al.* Low Emittance, High Brilliance Relativistic Electron Beams from a Laser-Plasma Accelerator. *Phys. Rev. Lett.* **105**, 215007 (2010). URL `http://link.aps.org/doi/10.1103/PhysRevLett.105.215007`

[21] Sears, C. M. S. *et al.* Emittance and divergence of laser wakefield accelerated electrons. *Phys. Rev. ST Accel. Beams* **13**, 092803 (2010). URL `http://link.aps.org/doi/10.1103/PhysRevSTAB.13.092803`

[22] Debus, A. D. *et al.* Electron Bunch Length Measurements from Laser-Accelerated Electrons Using Single-Shot THz Time-Domain Interferometry. *Phys. Rev. Lett.* **104**, 084802 (2010).

[23] van Tilborg, J. *et al.* Temporal Characterization of Femtosecond Laser-Plasma-Accelerated Electron Bunches Using Terahertz Radiation. *Phys. Rev. Lett.* **96**, 014801 (2006). URL `http://link.aps.org/doi/10.1103/PhysRevLett.96.014801`

[24] Buck, A. *et al.* Real-time observation of laser-driven electron acceleration. *Nature Physics* **7**, 543–548 (2011). URL `http://dx.doi.org/10.1038/nphys1942`

[25] Lundh, O. *et al.* Few femtosecond, few kiloampere electron bunch produced by a laser-plasma accelerator. *Nature Physics* **7**, 219–222 (2011).

[26] Leemans, W. P. *et al.* GeV electron beams from a centimetre-scale accelerator. *Nature Physics* **2**, 696–699 (2006).

[27] Wang, X. *et al.* Quasi-monoenergetic laser-plasma acceleration of electrons to 2 GeV. *Nature Communications* **4** (2013).